YITP-SB-01-35
BNL-HET-01/23
October 2, 2001

Energy Flow in Interjet Radiation

Carola F. Berger[a], Tibor Kúcs[a] and George Sterman[a,b]

[a] *C.N. Yang Institute for Theoretical Physics, SUNY Stony Brook*
Stony Brook, New York 11794 – 3840, U.S.A.

[b] *Physics Department, Brookhaven National Laboratory*
Upton, New York 11973, U.S.A.

Abstract

We calculate the distribution of transverse energy, Q_Ω, radiated into an arbitrary interjet angular region, Ω, in high-p_T two-jet events. We find a distribution that can be extrapolated smoothly to $Q_\Omega = \Lambda_{\rm QCD}$, where it vanishes. This method provides a class of predictions on transverse energy radiated between jets, as a function of jet energy and rapidity, and of the choice of the region Ω in which the energy is measured.

1. Introduction

Jet events at hadron colliders encode QCD time evolution over a large range of length scales, from the momentum transfer that produced the jets, to the scale of hadronization. They thus afford a window to the transition of quantum chromodynamics from short to long distances, in addition to being our most direct probe of new physics at short distances. In this paper, we will study transverse energy flow into specified angular regions between high-p_T jets. We will find a

variety of perturbative predictions, in which soft radiation is sensitive to color and flavor flow at short distances. The flow in soft radiation also has an impact on the comparison of measured cross sections in a hadronic environment to perturbative calculations. These measurements rely on our determination of the energies of jets in the presence of an "underlying event", consisting of particles not directly associated with jet production. Because jet cross sections fall so rapidly with momentum transfer, they are sensitive to relatively small shifts in energy [1, 2], even at the highest p_T. This is the case, even though the effects of such shifts are power-suppressed in p_T, compared to finite-order perturbative calculations. An understanding of the underlying event requires good control over perturbative bremsstrahlung associated with the hard scattering itself, so that the two effects may be separated.

The influence of the underlying event on jet energy measurements is a complex issue [3, 4, 5]. In the absence of further information, it is tempting to think of the particle production underlying the jets as similar to that in a minimum bias event, one in which there is no distinguishing hard scattering. Energy flow between jets in the final state, however, may result from multiple parton interactions [6, 7], which may or may not be the same in jet and minimum bias events, as well as from perturbative QCD bremsstrahlung associated with the hard scattering itself [8, 9]. Marchesini and Webber [10] argued that it should be possible to disentangle the underlying event from the bremsstrahlung of the hard scattering by studying the flow of transverse energy away from the jet direction. They pointed out that the average transverse energy of radiation into specified angular regions is infrared safe. We will develop here a further technique to compute the *distribution* in transverse energy of this radiation.

The other motivation for this study of interjet radiation is the light it may shed on short-distance color and flavor flow, and on the dynamics of hadronization. The relation of the angular dependence of interjet particle multiplicity to color flow in the hard scattering has been well-established in e^+e^- annihilation [11]. Its use in the analysis of jet events in hadronic scattering, to distinguish new physics signals from QCD background, was explored in [12, 13], and the method was verified experimentally in [14], through the analysis of events involving jets and W bosons. Here we shall follow [10], and investigate transverse energy flow rather than multiplicity, but the spirit of the approach is much the same.

The discussion below is also closely related to the treatment of rapidity gap ("color singlet exchange") events in Refs. [15, 16], for jets at high p_T and large rapidity separations. In this case, we will study relatively central pairs of jets, with the high-p_T tail of the inclusive jet cross section in mind. Correspondingly, we restrict ourselves to a valence approximation.

We will calculate the distribution for the flow of transverse energy, Q_Ω, radiated into a specific detector region, Ω, away from a set of observed jets. This is what we mean by interjet radiation.[1] The distribution in Q_Ω is perturbatively calculable as a factorized cross section, although for $Q_\Omega \ll Q$, with Q the hard momentum transfer, the perturbative expansion will in general include contributions of order $\alpha_s^n \ln^n(Q_\Omega/Q)$. We shall resum such terms in a leading logarithmic approximation. The analysis is made possible by the incoherence of wide-angle soft gluon radiation from the internal evolution of jets, a property of QCD which plays an important

[1] In fact, our analysis can be applied to a class of kinematic quantities, including the energy itself. We choose to work with the transverse energy simply because of its boost invariance.

role both in proofs of factorization [18], and in the study of jet properties through the coherent branching formalism [19, 11]. The discussion in this paper will be restricted to cross sections with exactly two high-p_T jets.

We will see how interjet radiation, although independent of the details of the jets themselves, depends upon both flavor and color exchanges at the hard scattering, and we will show how to derive the distribution of events in terms of Q_Ω for each combination. The choice of Ω is free, so long as it does not include the observed jets. In this paper, we illustrate our method with the relatively simple choice of a region whose area is of order unity in the $\eta - \phi$ space of rapidity and azimuthal angle, outside of the beam-jet scattering plane. We reserve the extension to more general regions Ω and to the very important role of gluons in the initial state for forthcoming work [17].

In the following section, we discuss the class of interjet energy flow cross sections that we will study, starting from their collinear-factorized form. We describe the refactorization of hard-scattering functions into fully short-distance functions, dependent only on scales at the level of the large momentum transfer, $Q^2 \sim p_T^2$, and a set of "soft", but perturbatively calculable, functions, which describe evolution at scales intermediate between Q^2 and Q_Ω^2. To apply perturbation theory, of course, we must assume that Q_Ω is large compared to the scale at which the running coupling becomes strong: $Q_\Omega^2 \gg \Lambda^2_{\rm QCD}$. We show how this refactorization leads to renormalization group equations for the soft functions, and hence for their Q_Ω-dependence. These are matrix equations describing the mixing of color [20]. Section 3 deals with the determination of the anomalous dimension matrices that control this evolution. We show how, at leading logarithm, their calculation reduces to the evaluation of integrals over the phase space of radiation into Ω. In Section 4, we study specific distributions for scales relevant to Tevatron high-p_T two-jet events. We close with a brief discussion of our results, and prospects for future progress.

2. Factorization and Refactorization

2.1. Dijets and interjet observables

We will discuss inclusive cross sections involving dijet production in hadronic collisions:

$$A(p_A) + B(p_B) \to J_1(p_1) + J_2(p_2) + R_\Omega(Q_\Omega) + X\,, \tag{1}$$

where the jets J_i have high transverse momenta. In principle, the jet axes may be identified by any jet-finding convention, but we shall always define the jet energy by flow into some angular region, a "cone". In Eq. (1), R_Ω denotes radiation into a region Ω outside these jet cones. The quantity Q_Ω is a kinematic measure of the radiation into Ω. We may, as in Refs. [15, 16], take Q_Ω to be the energy of particles in Ω, but we may also take it to be the transverse energy. We inclusively sum over the radiation X outside the jets and Ω. The jets are characterized by their transverse momenta and pseudorapidity, $\eta = \ln(\cot(\theta/2))$, where θ is the angle with respect to the beam axis. We will consider two-jet final states for which

$$|\vec{p}_{T1}| \sim |\vec{p}_{T2}| \gg Q_\Omega \gg \Lambda_{\rm QCD}\,. \tag{2}$$

Thus, the interjet radiation, although energetic enough to be treated in perturbation theory, is assumed to be soft enough that we need not consider the recoil of the high-p_T jets.

Collinear factorization theorems [18] ensure that we may write any such cross section at fixed Q_Ω as a sum of convolutions of parton distribution functions ϕ (PDFs) that incorporate long-distance dynamics, with hard-scattering functions, ω, that summarize short-distance dynamics,

$$\begin{aligned}\frac{d\sigma_{AB}}{d\vec{p}_1\, dQ_\Omega} &= \sum_{f_A,f_B} \int dx_A\, dx_B\; \phi_{f_A/A}\left(x_A,\mu_F\right) \phi_{f_B/B}\left(x_B,\mu_F\right) \\ &\qquad \times \omega_{f_A f_B}\left(x_A p_A, x_B p_B, \vec{p}_1, Q_\Omega, \mu_F, \alpha_s(\mu_F)\right)\,, \end{aligned} \tag{3}$$

with factorization scale μ_F. The sum is over parton types, f_A, f_B. Corrections to this relation begin in general with powers of $\Lambda^2_{\rm QCD}/Q^2_\Omega$, due to multiple scattering of partons – part of the underlying event referred to above. Our analysis below, which begins with Eq. (3), is thus accurate up to such corrections, and requires the conditions (2). We take the renormalization scale equal to the factorization scale. Because in this paper we will emphasize ratios of cross sections rather than their size, fixing $\mu_{\rm ren} = \mu_F = p_T$ is meant to be taken as an indication of the order of these scales, rather than the promotion of a specific choice.

2.2. Refactorization of the partonic cross section

As stated above, we define the energies of high-p_T jets by the energy flowing into specified cones, while the region Ω in which we measure Q_Ω is outside these cones. Soft gluon emission outside the angular extent of the jets decouples from the kinematics of the hard scattering, and from the internal evolution of the jets [18, 19, 11]. As a result, we may express $\omega_{f_A f_B}$ in Eq. (3) as a sum of terms, each characterized by a definite number of jets produced at the hard scattering. To lowest order in α_s, only two jets are possible. Thus, at leading order, the production of the high-p_T jets is given by the set of Born-level $2 \to 2$ partonic processes, which we label f,

$$\mathrm{f}: \qquad f_A + f_B \to f_1 + f_2\,. \tag{4}$$

We distinguish $q\bar{q} \to q\bar{q}$ ($f_1 = q$) from $q\bar{q} \to \bar{q}q$ ($f_1 = \bar{q}$). We may now write the single-jet inclusive cross section at fixed Q_Ω as

$$\frac{d\sigma_{AB}}{d\eta dp_T dQ_\Omega} = \sum_{\rm f} \int dx_A dx_B\; \phi_{f_A/A}\left(x_A,\mu_F\right) \phi_{f_B/B}\left(x_B,\mu_F\right)\; \delta\left(p_T - \frac{\sqrt{\hat{s}}}{2\cosh\hat{\eta}}\right)\; \frac{d\hat{\sigma}^{(\rm f)}}{d\hat{\eta} dQ_\Omega}\,, \tag{5}$$

with $\hat{\eta} = \eta - (1/2)\ln(x_A/x_B)$ the jet rapidity in the partonic center-of-mass, and $\hat{s} = x_A x_B s$. We neglect the effects of recoil of the observed jet against relatively soft radiation. The short-distance function $d\hat{\sigma}^{(\rm f)}/d\hat{\eta} dQ_\Omega$ is an expansion in $\alpha_s(p_T)$ that begins with the lowest order (LO) cross section,

$$\frac{d\hat{\sigma}^{(\rm f)}}{d\hat{\eta} dQ_\Omega} = \frac{d\hat{\sigma}^{(\rm f,LO)}}{d\hat{\eta}}\,\delta(Q_\Omega) + \ldots\,, \tag{6}$$

but which includes potentially large corrections associated with logarithms of Q_Ω/p_T. In the two-jet approximation described above, we work at leading order in the hard scattering, with the

factorization scale $\mu_F = p_T$. The sum runs over all possible partonic subprocesses f, defined as in (4). We emphasize that corrections to Eq. (5) begin at $\mathcal{O}(\alpha_s(p_T))$, due to processes with more than two energetic jets in the final state. Taking these into account would require generalizing the set of flavor flows f in Eq. (4) to $2 \to 3$ and beyond. Such a development will be informative, but we shall not pursue it here.

The hard-scattering function for the subprocess f may now be refactorized [21, 20], to exhibit the interrelation between the partonic hard scattering and soft radiation outside all jet cones. For this purpose, it is convenient to treat the partonic and hadronic cross sections integrated over the transverse energy radiated into region Ω, up to a fixed value Q_Ω,

$$\begin{aligned}
\frac{d\hat{\sigma}^{(\mathrm{f})}\left(p_T, \hat{\eta}, \mu_F, \alpha_s(\mu_F), Q_\Omega\right)}{d\hat{\eta}} &= \int_0^{Q_\Omega} dQ'_\Omega \frac{d\hat{\sigma}^{(\mathrm{f})}\left(p_T, \hat{\eta}, \mu_F, \alpha_s(\mu_F), Q'_\Omega\right)}{d\hat{\eta} dQ'_\Omega} \\
\frac{d\sigma_{AB}\left(p_T, \eta, \mu_F, \alpha_s(\mu_F), Q_\Omega\right)}{d\eta dp_T} &= \sum_{\mathrm{f}} \int dx_A dx_B \; \phi_{f_A/A}(x_A, \mu_F)\, \phi_{f_B/B}(x_B, \mu_F) \\
&\qquad \times \delta\left(p_T - \frac{\sqrt{\hat{s}}}{2\cosh\hat{\eta}}\right) \frac{d\hat{\sigma}^{(\mathrm{f})}\left(p_T, \hat{\eta}, \mu_F, \alpha_s(\mu_F), Q_\Omega\right)}{d\hat{\eta}} \,. \quad (7)
\end{aligned}$$

As we shall show, the relevant refactorization of the hard scattering function of Eq. (7) is

$$\frac{d\hat{\sigma}^{(\mathrm{f})}\left(p_T, \hat{\eta}, \mu_F, \alpha_s(\mu_F), Q_\Omega\right)}{d\hat{\eta}} = \sum_{L,I} H_{IL}^{(\mathrm{f})}\left(p_T, \hat{\eta}, \mu, \mu_F, \alpha_s(\mu)\right) S_{LI}^{(\mathrm{f})}\left(\hat{\eta}, \Omega, \frac{Q_\Omega}{\mu}, \alpha_s(\mu)\right) , \quad (8)$$

where $H_{IL}^{(\mathrm{f})}$ is a matrix of short-distance functions, independent of Q_Ω, while all of the Q_Ω-dependence is factored into dimensionless soft functions $S_{LI}^{(\mathrm{f})}$. Here μ is a new refactorization scale, chosen between p_T and Q_Ω, with dynamics on scales below μ incorporated into $S^{(\mathrm{f})}$. The soft function is independent of μ_F, which separates $d\hat{\sigma}/d\hat{\eta}$ from the parton distribution functions. The functions $S_{LI}^{(\mathrm{f})}$, which summarize dynamics of partons with energies at the scale Q_Ω, depend in general on the scalar products $\beta_i \cdot \beta_j$ between the lightlike 4-velocities of the incoming and outgoing energetic partons in the hard scattering, which radiate soft gluons. If we fix the scattering plane such that jet 1 is located at $\phi = 0$, the kinematics of two-to-two scattering reduces this dependence to a single variable, which we may take as $\hat{\eta}$, the rapidity of parton 1 (see Eq. (4)) in the partonic center-of-mass (c.m.) frame.

In Eq. (8), the hard-scattering functions H_{IL} begin at order α_s^2, while the soft functions S_{LI} begin at zeroth order. To leading logarithm, we need only these lowest-order contributions, denoted below as $H^{(\mathrm{f},\,1)}$ and $S^{(\mathrm{f},\,0)}$, respectively. The combination of these approximations is related to the lowest-order cross section by Eq. (6),

$$\frac{d\hat{\sigma}^{(\mathrm{f,LO})}}{d\hat{\eta}} = \sum_{L,I} H_{IL}^{(\mathrm{f},\,1)}\left(p_T, \hat{\eta}, \alpha_s(\mu_F)\right) S_{LI}^{(\mathrm{f},\,0)} \,. \quad (9)$$

Recalling that we expect corrections to Eq. (5) to begin at NLO in $\alpha_s(p_T)$ for inclusive jet production, Eq. (8) should hold to a corresponding accuracy in the hard-scattering function H_{IL}.

Additional corrections to the refactorization (8) may be due to multiple scattering. These corrections are suppressed by powers of $\Lambda^2_{\rm QCD}/Q^2_\Omega$. At large Q_Ω, therefore, bremsstrahlung dominates the inclusive cross section. At low Q_Ω, the NLO differential cross section for bremsstrahlung diverges as $1/Q_\Omega$. As we shall see, however, the resummed *integrated* cross section, Eq. (7), is better behaved, and may be extrapolated smoothly as far down as $Q_\Omega = \Lambda_{\rm QCD}$, where it vanishes. In these terms, the perturbative component of interjet radiation, which dominates for hard radiation, joins smoothly to the region of low radiation, and may thus be meaningfully compared to data [10].

2.3. The soft function

The proof of Eq. (8) at the desired accuracy, leading logarithm in Q_Ω, follows standard arguments in factorization [18, 22]. An essential ingredient in proofs of collinear factorization is that wide-angle soft radiation decouples from jet evolution [23]. Soft radiation away from jet directions is equally well described by radiation from a set of path-ordered exponentials – nonabelian phase operators or Wilson lines – that replace each of the partons involved in the hard scattering (four, in our case),

$$\begin{aligned}
\Phi^{(f)}_\beta(\infty,0;x) &= P\exp\left(-ig\int_0^\infty d\lambda\ \beta\cdot A^{(f)}(\lambda\beta+x)\right)\ , \\
\Phi^{(f')}_{\beta'}(0,-\infty;x) &= P\exp\left(-ig\int_{-\infty}^0 d\lambda\ \beta'\cdot A^{(f')}(\lambda\beta'+x)\right)\ ,
\end{aligned} \tag{10}$$

where P denotes path ordering. The first line describes an outgoing, and the second an incoming, parton, whose flavors and four-velocities are f and β, and f' and β', respectively. The vector potentials $A^{(f)}$ are in the color representation appropriate to flavor f, and similarly for $A^{(f')}$.

Because wide-angle, soft radiation is independent of the internal jet evolution, products of nonabelian phase operators, linked at the hard scattering by a tensor in the space of color indices generate the same wide-angle radiation as the full jets. The general form for these operators, exhibiting their color indices, is

$$\begin{aligned}
W^{(\rm f)}_{I\,\{c_i\}}(x) &= \sum_{\{d_i\}} \Phi^{(f_2)}_{\beta_2}(\infty,0;x)_{c_2,d_2}\ \Phi^{(f_1)}_{\beta_1}(\infty,0;x)_{c_1,d_1} \\
&\quad\times \left(c^{(\rm f)}_I\right)_{d_2,d_1;d_A,d_B}\ \Phi^{(f_A)}_{\beta_A}(0,-\infty;x)_{d_A,c_A}\ \Phi^{(f_B)}_{\beta_B}(0,-\infty;x)_{d_B,c_B}\ .
\end{aligned} \tag{11}$$

The c_I are color tensors in a convenient basis. Examples will be given below. The perturbative expansions for these operators are in terms of standard eikonal vertices and propagators, and have been given in detail in Refs. [21, 20]. In these terms, we define $S_{LI}^{(\mathrm{f})}$ as [2]

$$S_{LI}^{(\mathrm{f})}\left(\hat{\eta},\Omega,\frac{Q_\Omega}{\mu},\alpha_s(\mu)\right) = \int_0^{Q_\Omega} dQ'_\Omega \sum_n \sum_{\{b_i\}} \delta(Q_\Omega^{(n)} - Q'_\Omega) \times \langle 0|\,\bar{T}\left[\left(W_L^{(\mathrm{f})}(0)\right)^\dagger_{\{b_i\}}\right]|n\rangle\langle n|\,T\left[W_I^{(\mathrm{f})}(0)_{\{b_i\}}\right]|0\rangle\,. \qquad (12)$$

The sum is over all states n whose transverse energy flow into Ω is restricted to equal Q'_Ω. The indices L and I refer to the color exchange at the hard scattering between the partons in reaction f, as built into the definitions of the W's, Eq. (11). The matrix elements in Eq. (12) require renormalization, and we may identify the corresponding renormalization scale with the refactorization scale of Eq. (8).

The Q_Ω-dependence of the matrix $S_{LI}^{(\mathrm{f})}$ in Eq. (12) is the same as in the full partonic cross section, up to corrections due to differences between the jets and the nonabelian phase operators. Radiation within the jets, however, is treated inclusively in the sum over final states in (12). As observed above, radiation outside the jet cone is emitted coherently by the entire jet [18, 19, 11]. Any logarithmic enhancements associated with (angular ordered) radiation within the jets, or with radiation collinear to the eikonal lines, are thus independent of Q_Ω, and cancel in the sum over states. This cancellation occurs at fixed momenta for all on-shell particles within the jets [24, 23]. As a result, in the leading logarithmic approximation, differences between the eikonal and exact cross sections are given by Q_Ω-independent expansions in $\alpha_s(\mu)$, which may be absorbed into the hard functions H_{LI}. The H's themselves are thus the coefficient functions that match the effective eikonal operators $W_I^{(\mathrm{f})}$ to the full theory. Therefore, Eq. (8), with the soft function defined as in Eq. (12), reproduces the Q_Ω-dependence of the original cross section, to leading logarithm, the level of the original collinear factorization form restricted to a $2 \to 2$ hard scattering, Eq. (5).

Beyond leading logarithm, the sums over I and L in the factorized hard scattering cross section, Eq. (8), must be generalized to include the possibility of $2 \to 3$ and other scattering processes, in which more lines emerge from the short-distance processes. These processes begin at one extra order in $\alpha_s(p_T)$, and hence at next-to-leading logarithm in Q_Ω. They would account for corrections in which soft radiation resolves more than the two outgoing partons at the hard scattering. To include these higher-order processes, we would generalize the $2 \to 2$ eikonal cross sections of $S_{LI}^{(\mathrm{f})}$ of Eq. (12) to $2 \to 3$, by including three (or more) outgoing eikonal lines in $W^{(\mathrm{f})}$, Eq. (11). An expansion of this sort, analogous to the operator product expansion, would also require us to modify our definition of the matrix elements of Eq. (12), to avoid double counting. This would in turn affect the renormalization of $S_{LI}^{(\mathrm{f})}$. Because such modifications begin only at subleading logarithms, however, we can safely neglect them here.

[2] This definition of $S^{(\mathrm{f})}$ differs slightly from that of Ref. [15, 21, 20], in that it is an integral over Q_Ω, rather than differential in Q_Ω.

2.4. Resummation for the soft function

The partonic cross section $\hat{\sigma}$ must be independent of the refactorization scale, μ in Eq. (8), at which the soft (but still perturbative) wide-angle radiation, sensitive only to overall color flow, and the truly short-distance dynamics are separated:

$$\mu \frac{d}{d\mu} \left[\frac{d\hat{\sigma}^{(\mathrm{f})}}{d\hat{\eta}} \right] = 0 \,. \tag{13}$$

This condition applied to the right-hand side of (8) leads to a renormalization group equation,

$$\left(\mu \frac{\partial}{\partial \mu} + \beta(g_s) \frac{\partial}{\partial g_s} \right) S^{(\mathrm{f})}_{LI} = - \left(\Gamma^{(\mathrm{f})}_S(\hat{\eta}, \Omega) \right)^\dagger_{LJ} S^{(\mathrm{f})}_{JI} - S^{(\mathrm{f})}_{LJ} \left(\Gamma^{(\mathrm{f})}_S(\hat{\eta}, \Omega) \right)_{JI} \,, \tag{14}$$

with, as usual, $g_s = \sqrt{4\pi\alpha_s}$. Here $\left(\Gamma^{(\mathrm{f})}_S(\hat{\eta}, \Omega) \right)_{IL}$ may be thought of as an anomalous dimension matrix, which depends on the geometry of the region Ω in which soft radiation is observed. Eq. (14) holds to leading logarithm in μ, and hence Q_Ω, consistent with the accuracy of the underlying factorizations, Eqs. (5) and (8). As shown, the anomalous dimension matrices, and their eigenvalues, depend on the c.m. rapidity, $\hat{\eta}$, of the partons that participate in the hard scattering. Equivalently, they depend upon $\hat{\theta}$, the scattering angle in the partonic center-of-mass. We always fix the observed jet at $\phi = 0$.

To solve Eq. (14), we go to a basis for the color matrices $c^{(\mathrm{f})}_I$ that diagonalizes $\Gamma^{(\mathrm{f})}_S(\hat{\eta}, \Omega)$, through a transformation matrix R,

$$\left(\Gamma^{(\mathrm{f})}_S(\hat{\eta}, \Omega) \right)_{\gamma\beta} \equiv \lambda^{(\mathrm{f})}_\beta(\hat{\eta}, \Omega) \delta_{\gamma\beta} = R^{(\mathrm{f})}_{\gamma I} \left(\Gamma^{(\mathrm{f})}_S(\hat{\eta}, \Omega) \right)_{IJ} R^{(\mathrm{f})\,-1}_{J\beta}, \tag{15}$$

where

$$\lambda^{(\mathrm{f})}_\beta(\hat{\eta}, \Omega) = \frac{\alpha_s}{\pi} \lambda^{(\mathrm{f},\,1)}_\beta(\hat{\eta}, \Omega) + \ldots \tag{16}$$

are the eigenvalues of $\Gamma^{(\mathrm{f})}_S(\hat{\eta}, \Omega)$. Here and below, Greek indices $\beta,\ \gamma$ indicate that a matrix is evaluated in the basis where the soft anomalous dimension has been diagonalized. Thus, for the soft and short-distance functions we also write,

$$\begin{aligned} S^{(\mathrm{f})}_{\gamma\beta} &= \left[\left(R^{(\mathrm{f})-1} \right)^\dagger \right]_{\gamma L} S^{(\mathrm{f})}_{LK} \left[R^{(\mathrm{f})-1} \right]_{K\beta} \\ H^{(\mathrm{f})}_{\gamma\beta} &= \left[R^{(\mathrm{f})} \right]_{\gamma K} H^{(\mathrm{f})}_{KL} \left[R^{(\mathrm{f})\dagger} \right]_{L\beta} . \end{aligned} \tag{17}$$

The transformation matrix $R^{(\mathrm{f})-1}$ is given by the eigenvectors of the anomalous dimension matrix,

$$\left(R^{(\mathrm{f})\,-1} \right)_{K\beta} \equiv \left(e^{(\mathrm{f})}_\beta \right)_K \,. \tag{18}$$

The solution to Eq. (14), which resums leading logarithms of Q_Ω/μ, is straightforward. We introduce a combination of eigenvalues of $\Gamma^{(\mathrm{f})}_S$, $E^{(\mathrm{f})}_{\gamma\beta}(\hat{\eta}, \Omega)$, given by

$$E^{(\mathrm{f})}_{\gamma\beta}(\hat{\eta}, \Omega) = \frac{2}{\beta_0} \left[\lambda^{(\mathrm{f},\,1)\star}_\gamma(\hat{\eta}, \Omega) + \lambda^{(\mathrm{f},\,1)}_\beta(\hat{\eta}, \Omega) \right] \,, \tag{19}$$

in terms of the lowest-order coefficient of the beta function, $\beta_0 = (11N_c - 2n_f)/3$, for N_c colors and n_f quark flavors. The soft function is then

$$\begin{aligned} S^{(\mathrm{f})}_{\gamma\beta}\left(\hat{\eta}, \Omega, \frac{Q_\Omega}{\mu}, \alpha_s(\mu)\right) &= S^{(\mathrm{f})}_{\gamma\beta}\left(\hat{\eta}, \Omega, 1, \alpha_s(Q_\Omega)\right) \, \exp\left[E^{(\mathrm{f})}_{\gamma\beta}(\hat{\eta}, \Omega) \int_\mu^{Q_\Omega} \frac{d\mu'}{\mu'} \left(\frac{\beta_0}{2\pi}\alpha_s(\mu')\right)\right] \\ &= S^{(\mathrm{f})}_{\gamma\beta}\left(\hat{\eta}, \Omega, 1, \alpha_s(Q_\Omega)\right) \left(\frac{\alpha_s(\mu)}{\alpha_s(Q_\Omega)}\right)^{E^{(\mathrm{f})}_{\gamma\beta}(\hat{\eta}, \Omega)} , \end{aligned} \tag{20}$$

where in the second form we have reexpressed the result in terms of one-loop running couplings. We now set the refactorization scale, μ, equal to the transverse momentum of the observed jet, p_T, and find, for the partonic cross section,

$$\begin{aligned} \frac{d\hat{\sigma}^{(\mathrm{f})}\left(p_T, \hat{\eta}, \mu_F, \alpha_s(\mu_F), Q_\Omega\right)}{d\hat{\eta}} &= \sum_{\beta,\,\gamma} H^{(\mathrm{f})}_{\beta\gamma}\left(p_T, \hat{\eta}, \alpha_s(\mu_F)\right) \\ &\quad \times S^{(\mathrm{f})}_{\gamma\beta}\left(\hat{\eta}, \Omega, 1, \alpha_s(Q_\Omega)\right) \left(\frac{\alpha_s(p_T)}{\alpha_s(Q_\Omega)}\right)^{E^{(\mathrm{f})}_{\gamma\beta}(\hat{\eta}, \Omega)} . \end{aligned} \tag{21}$$

At leading logarithm, we approximate $H^{(\mathrm{f})}$ by $H^{(\mathrm{f},1)}$ and $S^{(\mathrm{f})}$ by $S^{(\mathrm{f},0)}$, as observed above. Then, for $Q_\Omega = p_T$, this expression reduces to the Born cross section for inclusive jet production, as in Eq. (9). The corresponding differential cross section in Q_Ω, valid to leading logarithm, is

$$\begin{aligned} &Q_\Omega \frac{d\hat{\sigma}^{(\mathrm{f})}\left(p_T, \hat{\eta}, \mu_F, \alpha_s(\mu_F), Q_\Omega\right)}{d\hat{\eta} dQ_\Omega} \\ &\quad = \sum_{\beta,\gamma} H^{(\mathrm{f},\,1)}_{\beta\gamma}\left(p_T, \hat{\eta}, \alpha_s(\mu_F)\right) \; S^{(\mathrm{f},\,0)}_{\gamma\beta} \; E^{(\mathrm{f})}_{\gamma\beta}(\hat{\eta}, \Omega) \left[\frac{\beta_0\alpha_s(Q_\Omega)}{2\pi}\right] \left(\frac{\alpha_s(p_T)}{\alpha_s(Q_\Omega)}\right)^{E^{(\mathrm{f})}_{\gamma\beta}(\hat{\eta}, \Omega)} . \end{aligned} \tag{22}$$

For consistency, we must recover at lowest order the eikonal approximation to the complete $2 \to 3$ cross section at fixed Q_Ω from (22). We shall see how this result emerges in the following section, where we describe the calculation of the exponents $E^{(\mathrm{f})}_{\gamma\beta}$.

Once the matrix $R^{(\mathrm{f})-1}$, Eq. (18), is determined in a specific basis for color exchange, the soft and short-distance matrices in Eq. (22) are found by applying Eq. (17). The lowest-order soft matrices $S^{(\mathrm{f},\,0)}_{LK}$ reduce to color traces only, while at leading logarithm, the hard matrices $H^{(\mathrm{f},\,1)}_{KL}$ are given by squares of the corresponding leading-order partonic $2 \to 2$ amplitudes, projected onto the original color basis.

We are now ready to introduce a convenient measure of soft radiation into region Ω in our dijet events. Consider the ratio

$$\rho_{AB}(p_T, \eta, Q_\Omega, \Omega) = \frac{1}{d\sigma^{(\mathrm{LO})}_{AB}/d\eta dp_T} \, \frac{d\sigma_{AB}(p_T, \eta, Q_\Omega)}{d\eta dp_T} , \tag{23}$$

where the numerator is the inclusive hadronic cross section given in Eq. (7) above, and the denominator is the lowest-order dijet cross section for the same hadrons,

$$\frac{d\sigma_{AB}^{(\mathrm{LO})}}{d\eta dp_T} = \sum_{\mathrm{f}} \int dx_A dx_B \, \phi_{f_A/A}\left(x_A,\mu_F\right) \phi_{f_B/B}\left(x_B,\mu_F\right) \times \delta\left(p_T - \frac{\sqrt{\hat{s}}}{2\cosh\hat{\eta}}\right) \sum_{I,\,L} H_{IL}^{(\mathrm{f},\,1)}\left(p_T,\hat{\eta},\alpha_s(\mu_F)\right) S_{LI}^{(\mathrm{f},\,0)} \,. \tag{24}$$

Here we have used Eq. (9) to relate the LO hard-scattering function $\hat{\sigma}$, in collinear factorization, to the lowest-order, refactorized hard and soft functions, H and S. By comparing this expression with Eqs. (7) and (21) for the numerator in (23), we see that, so long as $\mathrm{Re}\, E_{\gamma\beta} > 0$, ρ_{AB} vanishes for small Q_Ω (strictly speaking, at $Q_\Omega = \Lambda_{\mathrm{QCD}}$), increases monotonically with Q_Ω, and reaches unity at $Q_\Omega = p_T$. This behavior, due to resummation, is to be contrasted with the corresponding NLO expression for the same quantity, which diverges toward minus infinity for vanishing Q_Ω, where the virtual contribution dominates. The quantity ρ_{AB} is a leading-logarithm description of the jet cross section, which predicts the distribution of bremsstrahlung into region Ω.

3. The Anomalous Dimension Matrices

We now turn to the calculation of the anomalous dimensions $\Gamma_S^{(\mathrm{f})}$, introduced in Eq. (14) above. Equation (14), in turn, followed directly from the refactorization of the hard-scattering function, Eq. (8). The refactorization scale, μ of Eq. (8) was identified with the renormalization scale for the operators W in the definition of the soft functions $S^{(\mathrm{f})}$, Eq. (12) . In this section, we shall derive these anomalous dimensions from the renormalization of the soft function. We will work in Feynman gauge.

The renormalization of multi-eikonal vertices has been discussed in some detail in Ref. [20], and we shall follow the method outlined there, with an important difference. In [20], the anomalous dimensions $\Gamma_S^{(\mathrm{f})}$ were computed in axial gauge, after dividing an eikonal scattering amplitude by eikonal self-energy functions. This extra factorization eliminated double poles in dimensional regularization, which are associated with collinear emission by the nonabelian phase operators. In axial gauge, these singularities appear only in self-energy diagrams. In the present case, such an extra factorization is not necessary, because $S_{LI}^{(\mathrm{f})}$, defined as in (12) is free of collinear singularities associated with the eikonal lines, after the sum over intermediate states. The remaining ultraviolet divergences in $S_{LI}^{(\mathrm{f})}$ may be compensated through local counterterms, just as in [20]. From these counterterms, we may simply read off the entries of the anomalous dimension matrix $\Gamma_S^{(\mathrm{f})}$ in an MS renormalization scheme.

Given the definition of the soft function, Eq. (12), the counterterms for S in Eq. (8) are calculated only after a sum over final states. They therefore depend on the choice of Ω, and the scattering angle of the underlying process. A technical problem with this renormalization process is that real-gluon radiation outside of Ω into the final states of Eq. (12) is unlimited in energy,

and diverges in the ultraviolet. These ultraviolet divergences cancel against virtual corrections, but their presence introduces a potential ambiguity. We resolve this ambiguity by using as our guiding principle the refactorization formula itself, Eq. (8). We seek a renormalized soft function in Eq. (12) that separates the dynamics of soft radiation from the hard-scattering functions entirely in terms of subtractions for virtual diagrams, to produce short-distance functions $H_{IL}^{(\mathrm{f})}$ that are free of dependence on soft radiation, at all momentum scales less than or equal to μ, the refactorization scale.

As μ changes, the cancellation between real-gluon emission outside region Ω of $S_{LI}^{(\mathrm{f})}$, with an analogous portion of the virtual corrections, remains unaffected, because there is no cutoff on radiation outside Ω in the definition of $S_{LI}^{(\mathrm{f})}$. As observed above, however, enhancements associated with radiation outside of Ω cancel in the sum over states. This radiation therefore produces no dependence on the refactorization scale. Thus, no subtraction is necessary for it in the construction of the short-distance function. We are therefore able to renormalize $S_{LI}^{(\mathrm{f})}$ purely in terms of local counterterms for the vertices c_I and c_L^*, just as in Ref. [20], to one loop in renormalization constants, and therefore to leading logarithm in μ. The following two subsections describe the one-loop calculation of $S_{LI}^{(\mathrm{f})}$ in this approach.

3.1. Renormalization and color mixing

To begin, we consider the diagrams shown in Fig. 1. Figs. 1a and 1c are virtual corrections, while 1b shows the corresponding diagrams for real gluon emission. To compute the counterterms associated with these diagrams, we fix the transverse energy flow $Q_\Omega = 0$ in Eq. (12). Because the definition of the soft function is fully inclusive outside of region Ω, Fig. 1b contributes even at this point, when the gluon is emitted in any direction outside of Ω.

As is characteristic of eikonal diagrams, Figs. 1a-c are all proportional to scaleless integrals, which vanish in dimensional regularization. At $Q_\Omega = 0$, therefore, $S_{LI}^{(\mathrm{f},1)}$ is given entirely by its one-loop counterterms, which we denote as [21]

$$\begin{aligned} S_{LJ}^{(\mathrm{f},1)}\left(\hat{\eta},\Omega,0,\alpha_s(\mu),\varepsilon\right) &= -\left(Z_S^{(\mathrm{f},1)}\left(\hat{\eta},\Omega,\alpha_s(\mu),\varepsilon\right)\right)^\dagger_{LI} S_{IJ}^{(\mathrm{f},0)} \\ &\quad -S_{LI}^{(\mathrm{f},0)}\left(Z_S^{(\mathrm{f},1)}\left(\hat{\eta},\Omega,\alpha_s(\mu),\varepsilon\right)\right)_{IJ}, \end{aligned} \tag{25}$$

where $S^{(0)}$ is the zeroth order matrix, which, by Eq. (12) is a set of color factors, independent of $\hat{\eta}$ and Ω. The elements of Z are computed in $D = 4 - \varepsilon$ dimensions. It is important to note that the ε poles, given by the one-loop counterterms, have the interpretation of *infrared*, rather than ultraviolet, divergences in $S_{LI}^{(\mathrm{f})}$, and that they cancel infrared divergences from real-gluon emission into region Ω.[3] Following the standard analysis, the one-loop anomalous dimensions are given by

$$\left(\Gamma_S^{(\mathrm{f})}(\hat{\eta},\Omega)\right)_{IJ} = -\alpha_s \frac{\partial}{\partial \alpha_s}\,\mathrm{Res}_{\varepsilon\to 0}\left(Z_S^{(\mathrm{f},1)}\left(\hat{\eta},\Omega,\alpha_s(\mu),\varepsilon\right)\right)_{IJ}. \tag{26}$$

[3]More specifically, the divergences from virtual diagrams are proportional to $\delta(Q'_\Omega)$ in (12), and cancel real-gluon emission as integrable distributions.

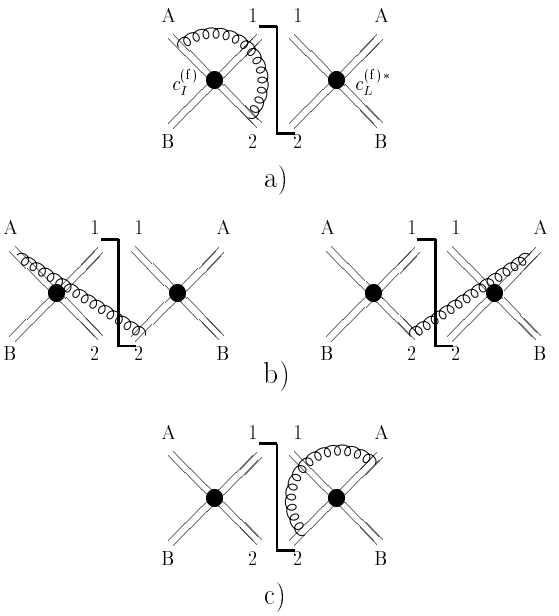

Figure 1: Diagrams for the calculation of the anomalous dimension matrix, as in Eq. (39). The double lines represent eikonal propagators, linked by vertices $c_I^{(\mathrm{f})}$ and $c_L^{(\mathrm{f})*}$, in the amplitude and its complex conjugate. The vertical line represents the final state.

The calculation of the Z's is thus essentially equivalent to the calculation of the anomalous dimensions. To carry out these calculations, however, we must specify a basis of color tensors, c_I.

For the two-to-two partonic processes, Eq. (4), we denote by r_i the color index associated with parton (or eikonal line) $i = A, B, 1, 2$. As above, capital letters, $I, J \ldots$ are indices in the space of color exchanges, spanned by a chosen basis for each partonic process. We will restrict the discussion here to the calculation of anomalous dimensions when the incoming partons are quarks or antiquarks. Convenient bases for describing the color flow for quark processes are t-channel singlet-octet bases, given by

$$\begin{aligned} c_1 &= \delta_{r_A,r_1}\delta_{r_B,r_2}, \\ c_2 &= -\frac{1}{2N_c}\delta_{r_A,r_1}\delta_{r_B,r_2} + \frac{1}{2}\delta_{r_A,r_B}\delta_{r_1,r_2} \end{aligned} \tag{27}$$

for $q\bar{q} \to q\bar{q}$, and

$$\begin{aligned} c_1 &= \delta_{r_A,r_1}\delta_{r_B,r_2}, \\ c_2 &= -\frac{1}{2N_c}\delta_{r_A,r_1}\delta_{r_B,r_2} + \frac{1}{2}\delta_{r_A,r_2}\delta_{r_B,r_1}. \end{aligned} \tag{28}$$

for $qq \to qq$. The process $q\bar{q} \to gg$ is best described in terms of the color basis

$$c_1 = \delta_{r_1,r_2}\,\delta_{r_A,r_B},$$

$$
\begin{aligned}
c_2 &= d_{r_2 r_1 c} \left(T_F^c\right)_{r_B r_A} , \\
c_3 &= i f_{r_2 r_1 c} \left(T_F^c\right)_{r_B r_A} ,
\end{aligned}
\tag{29}
$$

where c_1 is the s-channel singlet tensor, and c_2 and c_3 are the symmetric and antisymmetric octet tensors, respectively. Bases for other possible partonic processes with gluon eikonal lines have been given, for example, in Refs. [20, 16].

Let $Z^{(ij)}$ denote the contribution to the counterterms from all the one-loop graphs in which the gluon connects eikonal lines i and j. In this notation, the calculation of Fig. 1 gives us $Z^{(A2)}$. We emphasize that the Z's, and hence the anomalous dimensions, are to be calculated only after combining real-gluon emission diagrams with virtual diagrams. The Z's are constructed to give local counterterms that cancel only those ultraviolet divergences that are left over after the real-virtual cancellation has been carried out.

To find the $Z_{IJ}^{(ij)}$'s in the color bases (27) and (28), we rewrite the various one-loop virtual diagrams in terms of the original color basis, using the identity shown in Fig. 2,

$$
T_{ij}^a T_{kl}^a = \frac{1}{2} \left(\delta_{il} \delta_{jk} - \frac{1}{N_c} \delta_{ij} \delta_{kl} \right)
\tag{30}
$$

for quark processes. For scattering processes involving gluons, many useful identities can be found, for example, in [25]. This procedure results in a 2×2 matrix decomposition for scattering involving only quark and antiquark eikonal lines, describing the mixing under renormalization of their color exchanges. The annihilation of a pair of quark and antiquark eikonals into two gluon eikonal lines gives a 3×3 matrix structure, while for incoming and outgoing gluonic eikonals, we get an 8×8 matrix [20].

For a given $Z^{(ij)}$, the momentum-space integral appears as an overall factor. It is then convenient to introduce the notation

$$
\left(Z_S^{(ij)} \right)_{LI} = \zeta_{LI}^{(ij)} \, \omega^{(ij)} ,
\tag{31}
$$

where the ζ_{LI} are the coefficients that result from the color decomposition of the virtual diagram, and where the $\omega^{(ij)}$s include the ultraviolet pole part of the momentum space integral for the soft function S and remaining overall constants. Defined in this fashion, the sign of each $\omega^{(ij)}$ depends on the flow of flavor in the underlying process (see below). From (26) and (31) the relation between the ω's and the anomalous dimension matrices is

$$
\left(\Gamma_S^{(\mathrm{f})} \right)_{LI} = -\varepsilon \sum_{\{(ij)\}} \zeta_{LI}^{(ij)} \, \omega^{(ij)} .
\tag{32}
$$

As an example, we give the color decomposition of $\Gamma^{(A2)}$ in $q\bar{q} \to q\bar{q}$, for which we find, using Eq. (30),

$$
\zeta^{(A2)} = \begin{pmatrix} 0 & \frac{C_F}{2 N_c} \\ 1 & -\frac{1}{N_c} \end{pmatrix} .
\tag{33}
$$

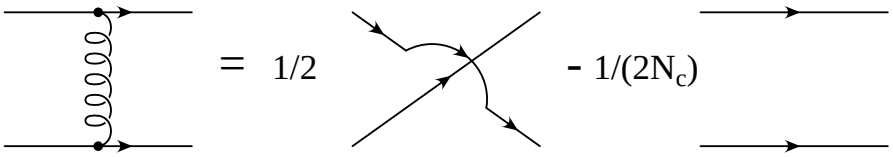

Figure 2: Color identity corresponding to Eq. (30).

The step to the anomalous dimensions is trivial, following Eqs. (26) and (32). We define

$$\Gamma^{(ij)} \equiv -\varepsilon\,\omega^{(ij)}\,. \tag{34}$$

Then we may summarize the full anomalous dimension matrices (32) in terms of the following combinations,

$$\begin{aligned}
\alpha^{(\mathrm{f})} &\equiv \Gamma^{(AB,\,\mathrm{f})} + \Gamma^{(12,\,\mathrm{f})},\\
\beta^{(\mathrm{f})} &\equiv \Gamma^{(A1,\,\mathrm{f})} + \Gamma^{(B2,\,\mathrm{f})},\\
\gamma^{(\mathrm{f})} &\equiv \Gamma^{(A2,\,\mathrm{f})} + \Gamma^{(B1,\,\mathrm{f})}.
\end{aligned} \tag{35}$$

In the basis (27), the anomalous dimension matrix for the process $q\bar{q} \to q\bar{q}$ is given by

$$\Gamma_S^{(q\bar{q}\to q\bar{q})} = \begin{pmatrix} C_F\beta^{(q\bar{q}\to q\bar{q})} & \frac{C_F}{2N_c}\left(\alpha^{(q\bar{q}\to q\bar{q})} + \gamma^{(q\bar{q}\to q\bar{q})}\right) \\ \alpha^{(q\bar{q}\to q\bar{q})} + \gamma^{(q\bar{q}\to q\bar{q})} & C_F\alpha^{(q\bar{q}\to q\bar{q})} - \frac{1}{2N_c}\left(\alpha^{(q\bar{q}\to q\bar{q})} + \beta^{(q\bar{q}\to q\bar{q})} + 2\gamma^{(q\bar{q}\to q\bar{q})}\right) \end{pmatrix}. \tag{36}$$

Here and below, we have suppressed the arguments of the momentum factors, α, β and γ for compactness, but they all depend on $\hat{\eta}$ and on Ω. The color decomposition for the process $q\bar{q} \to \bar{q}q$ is the same as above, Eq. (36). The momentum parts change, however: $\beta^{(q\bar{q}\to\bar{q}q)} = -\gamma^{(q\bar{q}\to q\bar{q})}$ and $\gamma^{(q\bar{q}\to\bar{q}q)} = -\beta^{(q\bar{q}\to q\bar{q})}$.

Similarly, for $qq \to qq$ in the basis (28), we have

$$\Gamma_S^{(qq\to qq)} = \begin{pmatrix} C_F\beta^{(qq\to qq)} & \frac{C_F}{2N_c}\left(\alpha^{(qq\to qq)} + \gamma^{(qq\to qq)}\right) \\ \alpha^{(qq\to qq)} + \gamma^{(qq\to qq)} & C_F\gamma^{(qq\to qq)} - \frac{1}{2N_c}\left(2\alpha^{(qq\to qq)} + \beta^{(qq\to qq)} + \gamma^{(qq\to qq)}\right) \end{pmatrix}. \tag{37}$$

Note that certain momentum factors for quark-quark and quark-antiquark differ by signs, due to the eikonal Feynman rules (see below, Sec. 3.2).

For $q\bar{q} \to gg$ we find in the basis (29),

$$\Gamma_S^{(q\bar{q}\to gg)} = \begin{pmatrix} C_F\Gamma^{(AB)} + C_A\Gamma^{(12)} & 0 & \frac{1}{2}(\beta+\gamma) \\ 0 & \xi & \frac{N_c}{4}(\beta+\gamma) \\ \beta+\gamma & \frac{N_c^2-4}{4N_c}(\beta+\gamma) & \xi \end{pmatrix}, \tag{38}$$

where $\xi \equiv \frac{N_c}{4}(\beta-\gamma) - \frac{1}{2N_c}\Gamma^{(AB)} + \frac{N_c}{2}\Gamma^{(12)}$. Here we have suppressed the superscripts, and define the $\Gamma^{(ij)}$, as well as α, β and γ for $q\bar{q} \to gg$ to be the same as those above for $q\bar{q} \to q\bar{q}$. We

have done so because, for processes involving gluons, the factorization into momentum and color factors as in (31) is ambiguous. The gluon-eikonal gluon vertex has both momentum and color parts, and the sign of each depends on the orientation with which the exchanged gluon attaches to the gluon eikonal line. Their product, and the anomalous dimension matrix, of course, is independent of the way the graphs are drawn.

3.2. Momentum integrals

We now compute the momentum integrals $\omega^{(ij)}$ that contribute to the matrix of renormalization constants $\left(Z_S^{(\mathrm{f})}\right)_{LI}$, at one loop, through Eq. (31). The momentum factor for the virtual diagram in which the gluon line connects eikonal lines i and j, such as Fig. 1a, may be written as [21, 20]

$$\omega_V^{(ij)}\left(\delta_i\beta_i, \delta_j\beta_j, \Delta_i, \Delta_j\right) \;=\; g_s^2 \int\limits_{P.P.} \frac{d^nk}{(2\pi)^n}\, \frac{-i}{k^2+i\epsilon}\, \frac{\Delta_i\Delta_j\beta_i\cdot\beta_j}{\left(\delta_i\beta_i\cdot k+i\epsilon\right)\left(\delta_j\beta_j\cdot k+i\epsilon\right)}\,, \tag{39}$$

where here and below the subscript $P.P.$ indicates that the integral is defined by its ultraviolet pole part. In (39), $\delta_i = 1(-1)$ for momentum k flowing in the same (opposite) direction as the momentum flow of line i, and $\Delta_i = 1(-1)$ for i a quark (antiquark) line, while, as noted above, we define the momentum integrals for gluons to have the same signs as for quark-antiquark scattering. For example, Fig. 1a for $q\bar{q} \to q\bar{q}$ has $i = \mathrm{A}$, $j = 2$, with $\Delta_A = 1$, $\Delta_2 = -1$ and with $\delta_A = \delta_2$. In this notation, each of the real gluon emission diagrams, such as in Fig. 1b, takes the form

$$\omega_R^{(ij)}\left(\delta_i\beta_i, \delta_j\beta_j, \Delta_i, \Delta_j\right) \;=\; g_s^2 \int\limits_{P.P.} \frac{d^nk}{(2\pi)^{n-1}}\, \delta_+(k^2)\, \left(1-\Theta(\vec{k})\right)\, \frac{\Delta_i\Delta_j\beta_i\cdot\beta_j}{\left(\delta_i\beta_i\cdot k\right)\left(\delta_j\beta_j\cdot k\right)}\,, \tag{40}$$

with δ_i and δ_j defined by the corresponding virtual diagram. The function $\Theta(\vec{k}) = 1$ when the vector $\vec{k}$ is directed into region Ω, and is zero otherwise. Both real-emission diagrams give the same answer, while the two virtual diagrams are complex conjugates of each other.

The sum of the virtual diagram in the amplitude with either of the real diagrams gives:

$$\begin{aligned}
\omega^{(ij)}\left(\delta_i\beta_i, \delta_j\beta_j, \Delta_i, \Delta_j\right) \;&=\; \omega_V^{(ij)} + \omega_R^{(ij)} \\
&=\; -g_s^2 \int\limits_{P.P.} \frac{d^nk}{(2\pi)^{n-1}}\, \delta_+(k^2)\, \Theta(\vec{k})\, \frac{\Delta_i\Delta_j\beta_i\cdot\beta_j}{\left(\delta_i\beta_i\cdot k\right)\left(\delta_j\beta_j\cdot k\right)} \\
&\qquad +\Delta_i\Delta_j\delta_i\delta_j\, \frac{\alpha_s}{2\pi}\, \frac{i\pi}{\varepsilon}\, \left(1-\delta_i\delta_j\right) \\
&\equiv\; -\frac{\Gamma^{(ij)}}{\varepsilon}\,.
\end{aligned} \tag{41}$$

In the last line, we have recalled the definition (34). The term with the k-integral is the real remainder of the cancellation of the real and virtual diagrams, while the imaginary part is nonzero only for $(ij) = (12)$ or (AB). At $Q_\Omega = 0$, the real diagrams $\omega_R^{(ij)}$ get contributions only from

gluon emission outside of Ω, and cancel contributions from $\omega_V^{(ij)}$ as shown in Eq. (41). The counterterms are identified after this cancellation has been carried out, and are implemented as local subtractions at the color vertices, c_I and c_L^*. This requires that the counterterms, and therefore the anomalous dimensions, be complex.

Given the anomalous dimensions computed in this fashion, and the lowest-order hard and soft functions, we find the differential cross section for interjet radiation into region Ω from Eq. (22). Note that for $Q_\Omega \neq 0$, the cross section may be fixed uniquely at one loop by the condition that the integral of the real part down to $Q_\Omega = 0$ must cancel the divergences of the virtual diagrams, that is, the counterterms identified above. We recognize that the result is consistent with Eq. (22) expanded to one loop, after a transformation to the diagonal basis for color exchange. The inclusive cross sections are given similarly, by Eq. (21).

4. Out-of-plane Radiation

As an illustration of our method, we introduce a region Ω that is fixed out of the scattering plane, as a "rectangular patch" in the space of rapidity y and azimuthal angle ϕ. Other choices are possible of course, and will be explored elsewhere.

Taking the observed jet at $\phi = 0$, and the recoil jet at $\phi = \pi$, we define Ω in the hadronic center-of-mass frame by

$$\begin{aligned} \phi_{min} < \quad \phi \quad < \phi_{max} \,, \\ \eta_{min} < \quad y \quad < \eta_{max} \,, \end{aligned} \tag{42}$$

where the boundaries are chosen such that the patch is located outside the incoming beams and outgoing jets. The distribution of energy radiated into the out-of-plane patch is determined by the eigenvectors and eigenvalues of the anomalous dimension matrices, $\Gamma_S^{(\mathrm{f})}$, Eqs. (36), (37), and (38) above. Given the definition (42) for Ω, which is the phase space available for soft gluon radiation, and the expressions (41) for the diagrammatic contributions, we simply need to evaluate the one loop integrals over the loop momenta restricted to this phase space.

4.1. Entries for the anomalous dimensions

For the patch region of Eq. (42), all the phase space integrals of Eq. (41), and hence all the entries of the anomalous dimensions, $\Gamma_S^{(\mathrm{f})}$, in Eqs. (36)-(38) can be expressed in terms of the following combinations of logarithmic and dilogarithmic functions,

$$I(x,y,z) = \arctan(z)\,\ln\left(\frac{x+z}{y+z}\right) + \frac{1}{2i}\left\{\mathrm{Li}_2\left(\frac{x+z}{z+i}\right) + \mathrm{Li}_2\left(\frac{y+z}{z-i}\right)\right\} - \frac{1}{2i}\left\{x \leftrightarrow y\right\} . \tag{43}$$

We note that this function has a finite limit to $z = \pm i$, where singularities of the dilogarithms cancel those of the arctangent:

$$I(x,y,\pm i) = \frac{1}{\pm 2i}\left\{\frac{1}{2}\left[\ln^2\left(\frac{x\pm i}{\pm 2i}\right) - \ln^2\left(\frac{y\pm i}{\pm 2i}\right)\right] + \mathrm{Li}_2\left(\frac{x\pm i}{\pm 2i}\right) - \mathrm{Li}_2\left(\frac{y\pm i}{\pm 2i}\right)\right\} . \tag{44}$$

For the anomalous dimension matrices relevant in the valence quark approximation, we need explicit expressions for $\Gamma^{(AB,\,\mathrm{f})}$ and $\Gamma^{(12,\,\mathrm{f})}$, in addition to $\alpha^{(\mathrm{f})}$, $\beta^{(\mathrm{f})}$ and $\gamma^{(\mathrm{f})}$, defined in Eq. (35). With variables in (42) transformed to the partonic center-of-mass frame, the relevant arguments of the I's in Eq. (43-44) are:

$$\begin{aligned}
x_{min} &= \tanh\left(\frac{\hat{\eta}+\hat{\eta}_{min}}{2}\right)\,\tan(\phi_{max}/2),\\
x_{max} &= \tanh\left(\frac{\hat{\eta}+\hat{\eta}_{max}}{2}\right)\,\tan(\phi_{max}/2),\\
y_{min} &= \coth\left(\frac{\hat{\eta}-\hat{\eta}_{min}}{2}\right)\,\tan(\phi_{max}/2),\\
y_{max} &= \coth\left(\frac{\hat{\eta}-\hat{\eta}_{max}}{2}\right)\,\tan(\phi_{max}/2),\\
z &= -\frac{\sinh(\hat{\eta})+i}{\cosh(\hat{\eta})}\,\tan(\phi_{max}/2).
\end{aligned} \tag{45}$$

In these terms, we have

$$\begin{aligned}
\frac{2\pi^2}{\alpha_s}\,\Gamma^{(AB,\,q\bar{q}\to q\bar{q})} &= (\hat{\eta}_{max}-\hat{\eta}_{min})(\phi_{max}-\phi_{min}) - 2\pi^2 i,\\
\frac{2\pi^2}{\alpha_s}\,\Gamma^{(12,\,q\bar{q}\to q\bar{q})} &= \{\, I(x_{min},x_{max},0) - I(x_{min},x_{max},z) - I(x_{min},x_{max},z^*)\,\} - \{\phi_{max}\to\phi_{min}\}\\
&+ \{\, -I(y_{min},y_{max},0) + I(y_{min},y_{max},z) + I(y_{min},y_{max},z^*)\,\} - \{\phi_{max}\to\phi_{min}\}\\
&- 2\pi^2 i,\\
\frac{2\pi^2}{\alpha_s}\,\beta^{(q\bar{q}\to q\bar{q})} &= \{I(-y_{min},-y_{max},0) - 2\,I(-y_{min},-y_{max},-\tan(\phi_{max}/2))\} - \{\phi_{max}\to\phi_{min}\}\\
&+ \{I(x_{min},x_{max},0) - 2\,I(x_{min},x_{max},\tan(\phi_{max}/2))\} - \{\phi_{max}\to\phi_{min}\}\,,
\end{aligned} \tag{46}$$

while $\gamma^{(q\bar{q}\to q\bar{q})}$ is found from $\beta^{(q\bar{q}\to q\bar{q})}$ through the transformation,

$$\gamma^{(q\bar{q}\to q\bar{q})}(\hat{\eta}_{min},\hat{\eta}_{max},\phi_{min},\phi_{max},\hat{\eta}) \;=\; \beta^{(q\bar{q}\to q\bar{q})}(-\hat{\eta}_{min},-\hat{\eta}_{max},\phi_{min},\phi_{max},-\hat{\eta})\,. \tag{47}$$

Expressions for quark-quark scattering differ only by overall signs, determined by the factors Δ_i in Eq. (41).

The anomalous dimension matrices are found by substituting these results into Eq. (36) for $q\bar{q}$ scattering into $q\bar{q}$, or (38) for their annihilation into gluons, or (37) for the quark-quark case. It is then straightforward to find the corresponding eigenvalues, $\lambda_\alpha^{(\mathrm{f})}$, Eq. (16), and transformation matrices $R^{(\mathrm{f})-1}$, Eq. (18). The results are somewhat cumbersome, and we do not present them here. In Figs. 3 and 4, we plot the real and imaginary parts of the exponents $E_{\alpha\beta}$, Eq. (19), for $q\bar{q}\to q\bar{q}$ and $q\bar{q}\to gg$, as functions of $\hat{\eta}$, the rapidity of the observed jet in the partonic center-of-mass, for a typical out-of-plane patch Ω, Eq. (42). For these plots we have chosen a configuration with $x_A = x_B$ in the factorization, Eq. (7), so that the partonic and hadronic c.m.

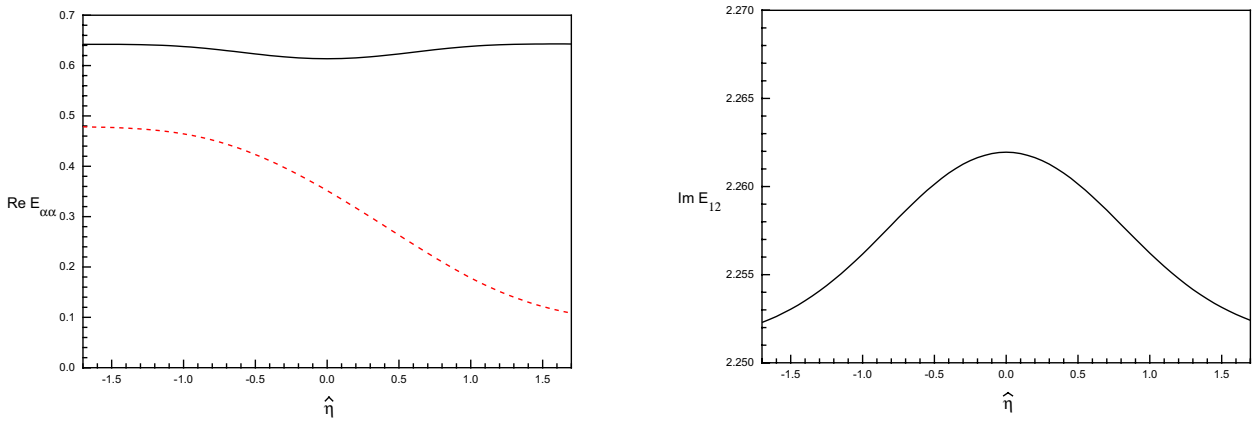

Figure 3: Real and imaginary parts of $E_{\alpha\beta}$ for $q\bar{q} \to q\bar{q}$ with Ω chosen as in Eq. (42), with $\phi_{min} = \pi/4$, $\phi_{max} = 3\pi/4$, and $\eta_{max} = -\eta_{min} = 1$. For the real parts we plot only the diagonal elements, Re $E_{\alpha\alpha}$, since the interference terms, Re $E_{\alpha\beta}$ with $\alpha \neq \beta$, are just the averages of the former. Note Im $E_{\alpha\alpha} = 0$, and that for an $n \times n$ anomalous dimension matrix, only $n - 1$ imaginary parts of the $E_{\alpha\beta}$ with $\alpha \neq \beta$ are independent.

frames coincide, with $\eta_{max} = -\eta_{min} = 1$, $\phi_{min} = \pi/4$ and $\phi_{max} = 3\pi/4$. Note that $E_{\alpha\beta}$ changes with x_A and x_B as Ω, fixed in the hadronic c.m., is boosted in the partonic c.m. The real parts of $E_{\alpha\beta}$ are all of order unity in the range of $\hat{\eta}$ shown. We expect them to be stable against higher-order corrections, so long as the size of the patch is of order unity. For very small patches, we would in general anticipate large logarithms associated with an incomplete cancellation between real and virtual corrections.

The only remaining ingredients necessary to compute the resummed cross sections, Eqs. (21) and (22) are the hard and soft functions at lowest order, to which we now turn.

4.2. Hard and soft matrices at LO

Explicit hard and soft matrices in color space at LO for the partonic processes $q\bar{q} \to q\bar{q}$ and $qq \to qq$ have been given in Ref. [16]. We exhibit them here, along with those for $q\bar{q} \to gg$, with a trivial change in overall normalization relative to [16]. To use them in the resummed cross sections, Eqs. (21) or (22), it is necessary to apply the transformation rules (17), to take the results quoted below to the Ω-dependent diagonal basis.

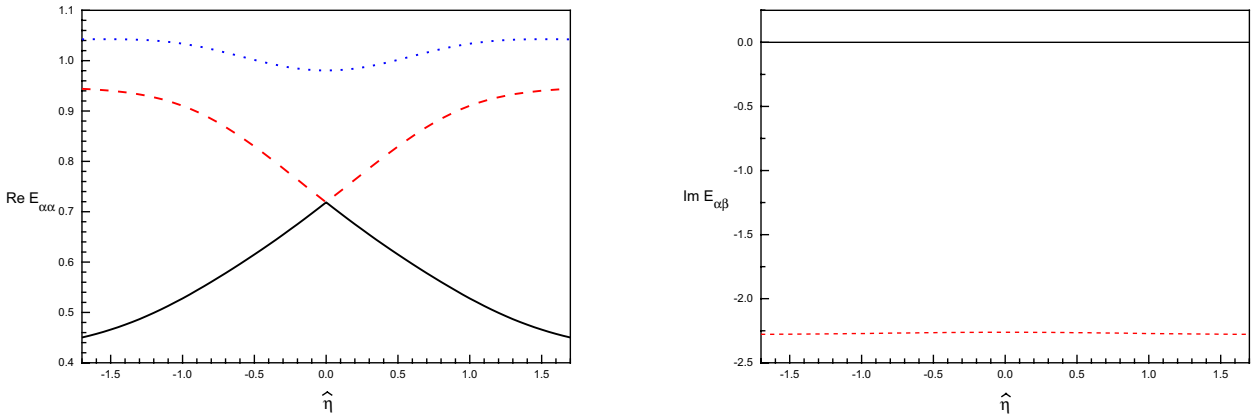

Figure 4: Real and imaginary parts of $E_{\alpha\beta}$ for $q\bar{q} \to gg$.

4.2.1. Hard and soft matrices for $q\bar{q} \to q\bar{q}$ at LO

In the basis (27) the decomposition of the Born level hard scattering for same-flavor $q\bar{q} \to q\bar{q}$ in color space is given by the matrix

$$H^{(1)}\left(\hat{t},\hat{s},\alpha_s\right) = \frac{1}{N_c^2}\frac{\pi\alpha_s^2}{\hat{s}}\frac{4\hat{t}\hat{u}}{\hat{s}^2}\begin{pmatrix} \left(\frac{C_F}{N_c}\right)^2\chi_1 & \frac{C_F}{N_c^2}\chi_2 \\ \frac{C_F}{N_c^2}\chi_2 & \chi_3 \end{pmatrix}, \tag{48}$$

where χ_1, χ_2, and χ_3 are defined by

$$\begin{aligned} \chi_1 &= \frac{\hat{t}^2+\hat{u}^2}{\hat{s}^2} \\ \chi_2 &= N_c\frac{\hat{u}^2}{\hat{s}\hat{t}} - \frac{\hat{t}^2+\hat{u}^2}{\hat{s}^2} \\ \chi_3 &= \frac{\hat{s}^2+\hat{u}^2}{\hat{t}^2} + \frac{1}{N_c^2}\frac{\hat{t}^2+\hat{u}^2}{\hat{s}^2} - \frac{2}{N_c}\frac{\hat{u}^2}{\hat{s}\hat{t}}. \end{aligned} \tag{49}$$

The step to the unequal-flavor cases, $q\bar{q}' \to q\bar{q}'$ and $q\bar{q} \to q'\bar{q}'$ is straightforward, by dropping the s-channel terms for the former, and the t-channel contributions for the latter. The matrix for $q\bar{q} \to \bar{q}q$ is found from (48) by exchanging $\hat{t}$ and $\hat{u}$. The lowest-order soft matrix is just given by the trace of the color basis, $S_{LI}^{(0)} = \text{Tr}\,(c_L^\dagger c_I)$, resulting in

$$S^{(0)} = \begin{pmatrix} N_c^2 & 0 \\ 0 & \frac{1}{4}(N_c^2-1) \end{pmatrix}. \tag{50}$$

4.2.2. Hard and soft matrices for $qq \to qq$ at LO

For this process we get, in the basis Eq. (28), a hard matrix related to the one for $q\bar{q} \to q\bar{q}$, Eq. (48), by the crossing transformation $\hat{s} \leftrightarrow \hat{u}$. The functions χ_1, χ_2 and χ_3 here are given by

$$\begin{aligned}
\chi_1 &= \frac{\hat{s}^2 + \hat{t}^2}{\hat{u}^2} \\
\chi_2 &= N_c \frac{\hat{s}^2}{\hat{t}\hat{u}} - \frac{\hat{s}^2 + \hat{t}^2}{\hat{u}^2} \\
\chi_3 &= \frac{\hat{s}^2 + \hat{u}^2}{\hat{t}^2} + \frac{1}{N_c^2} \frac{\hat{s}^2 + \hat{t}^2}{\hat{u}^2} - \frac{2}{N_c} \frac{\hat{s}^2}{\hat{t}\hat{u}} \,.
\end{aligned} \tag{51}$$

Again, $qq' \to qq'$ is found by keeping only the t-channel terms. The lowest-order soft matrix is the same as for $q\bar{q} \to q\bar{q}$.

4.2.3. Hard and soft matrices for $q\bar{q} \to gg$ at LO

In the basis (29), the Born level hard-scattering matrix is

$$H^{(1)}\left(\hat{t}, \hat{s}, \alpha_s\right) = \frac{1}{N_c^2} \frac{\pi \alpha_s^2}{\hat{s}} \frac{\hat{t}\hat{u}}{\hat{s}^2} \begin{pmatrix} \frac{1}{N_c^2}\chi_1 & \frac{1}{N_c}\chi_1 & \frac{1}{N_c}\chi_2 \\ \frac{1}{N_c}\chi_1 & \chi_1 & \chi_2 \\ \frac{1}{N_c}\chi_2 & \chi_2 & \chi_3 \end{pmatrix} , \tag{52}$$

where χ_1, χ_2, and χ_3 are now given by

$$\begin{aligned}
\chi_1 &= \frac{\hat{t}^2 + \hat{u}^2}{\hat{t}\hat{u}} \\
\chi_2 &= \left(1 + \frac{2\hat{t}}{\hat{s}}\right) \chi_1 \\
\chi_3 &= \left(1 - \frac{4\hat{t}\hat{u}}{\hat{s}^2}\right) \chi_1 \,.
\end{aligned} \tag{53}$$

The zeroth order soft matrix is found to be

$$S^{(0)} = C_F \begin{pmatrix} 2N_c^2 & 0 & 0 \\ 0 & N_c^2 - 4 & 0 \\ 0 & 0 & N_c^2 \end{pmatrix} . \tag{54}$$

4.3. Cross sections

Given the hard and soft functions, and the entries of the anomalous dimension matrices, we have all the ingredients necessary to calculate the inclusive cross section (21), its differential counterpart (22), and the ratio ρ, Eq. (23), for $p\bar{p}$ scattering in valence approximation. For a

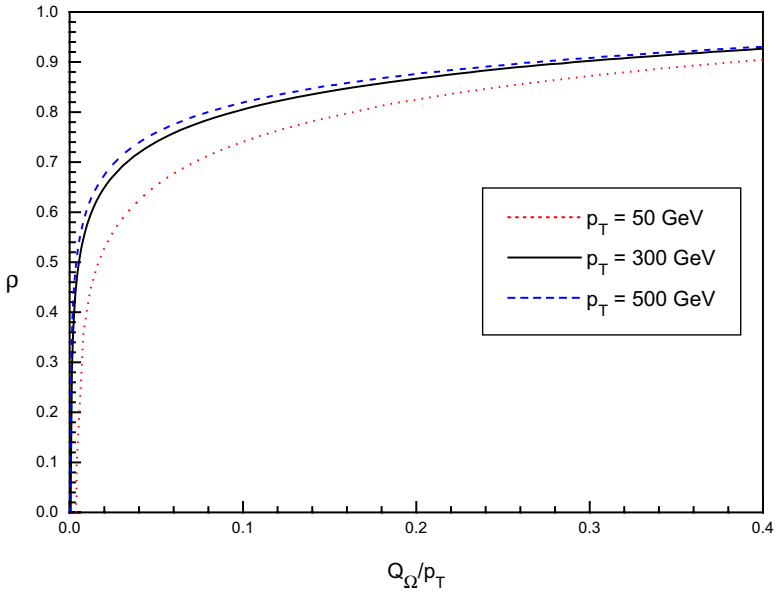

Figure 5: The distributions $\rho(x = Q_\Omega/p_T)$ for the region Ω defined in Sec. 4.1, with the observed jet at $\eta = 0$ with $\mu_F = p_T = 50$, 300 and 500 GeV. This calculation was carried out in valence quark approximation for $p\bar{p}$ scattering, at $\sqrt{s} = 1.8$ TeV.

given choice of Ω, such as the patch described above in terms of azimuthal angles and rapidities, we find first the functions $\Gamma^{(ij,\mathrm{f})}$, $\alpha^{(\mathrm{f})}$, $\beta^{(\mathrm{f})}$ and $\gamma^{(\mathrm{f})}$ for $(\mathrm{f}) = (q\bar{q} \to q\bar{q}), (q\bar{q} \to \bar{q}q), (q\bar{q} \to gg)$, as in Sec. 4.1. The resulting anomalous dimension matrices are given by Eqs. (36) and (38). We must diagonalize these matrices, finding eigenvalues λ_α, and the transformation matrices $R^{-1}_{I\beta}$, Eq. (18), which are used to take the hard and soft functions to the diagonal basis space, as in Eq. (17). Finally, the exponents $E_{\alpha\beta}$ that appear in the cross sections are found from Eq. (19).

As an example, we consider predictions for high-p_T jets at zero hadronic c.m. rapidity ($\eta = 0$) in $p\bar{p}$ scattering at $\sqrt{s} = 1.8$ TeV. We work in valence quark approximation, and therefore need only the exponents for quark-antiquark initial states. For Ω, we take the patch discussed in Sec. 4.1, whose exponents $E_{\alpha\beta}$ were plotted in Figs. 3 and 4. The resulting ratio ρ is shown in Fig. 5 for $p_T = 50$, 300 and 500 GeV as a function of $x = Q_\Omega/p_T$, the ratio of the transverse energy flow to p_T, for $0 < x < 0.4$. (We set ρ to zero below Λ_{QCD}.) For larger Q_Ω, we expect recoil, which we have not taken into account, to be important. In this calculation, we have chosen the renormalization and factorization scales equal to p_T, and have used CTEQ5L parton distribution functions [26]. The dependence of the ratio ρ on the choice of the factorization scale is very weak.

Recall that $\rho(x)$ measures the fraction of events for which the radiated transverse energy is less than or equal to xp_T. For any choice of Ω the real parts of the exponents E, Eq. (19), are positive. As a result, the ratio ρ vanishes for $Q_\Omega = \Lambda_{\mathrm{QCD}}$, and rises rapidly with x. For example, when $p_T = 500$ GeV, roughly 80% of events have $Q_\Omega < 50$ GeV for this choice of Ω. In addition,

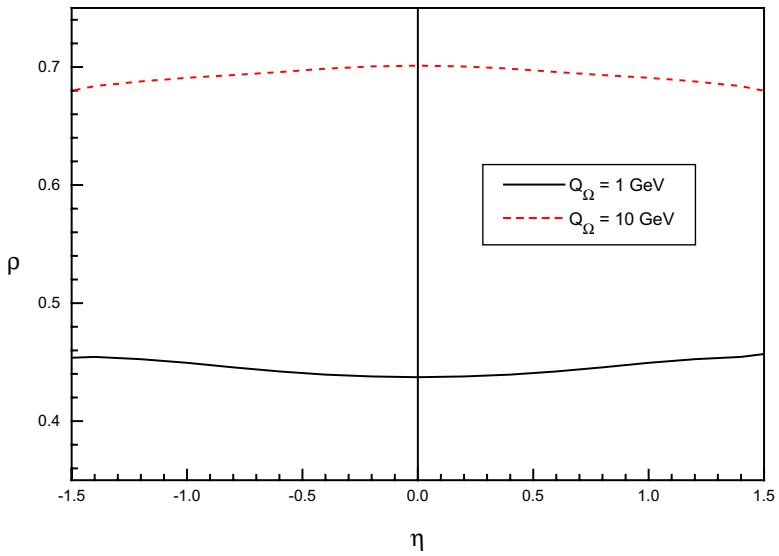

Figure 6: The η-dependence of $\rho(x)$ for a fixed region Ω defined as in Sec. 4.1., for radiated energies $Q_\Omega = 1$ GeV and 10 GeV, respectively, and $p_T = 300$ GeV.

for the choice of Ω given above, $\mathrm{Re}\, E_{\alpha\beta}$ is almost always less than unity, and the distribution $d\rho/dQ_\Omega$, found from Eqs. (23) and (22), actually diverges at $Q_\Omega = \Lambda_{\rm QCD}$. A similar behavior was found for "gap" dijet events, with low radiation in a large region that covers all $0 \leq \phi < 2\pi$ between high-p_T jets that are widely-separated in rapidity [15]. In such gap events there is an anomalously small eigenvalue, corresponding to a color exchange that approaches pure singlet in the t-channel for $\eta \to \infty$. In contrast, for the region Ω considered here, which is outside the scattering plane and of limited extent in rapidity, all the eigenvalues are relatively small.

The lowest-order expansion of the differential cross section $d\hat{\sigma}^{(\mathrm{f})}/d\hat{\eta}dQ_\Omega$, Eq. (22), corresponds to the eikonal approximation for the NLO correction to the cross section [10]. This cross section is proportional to the real parts of the exponents $E_{\alpha\beta}$, Eq. (19), and is hence proportional to the size of the region Ω in $\eta - \phi$ space. The vanishing of ρ at low energy flow is an expression of the tendency for the scattered quarks to radiate, essentially according to the "antenna pattern" [19, 11, 27] of the corresponding classical field. The divergence of the perturbative one-loop running coupling is responsible for the vanishing of $\rho(x)$ for $x = \Lambda_{\rm QCD}/p_T$ rather than at zero, as would be the case for a fixed coupling. The rapid rise in $\rho(x)$ indicates that most events generate relatively small amounts of perturbative radiation into the patch region. The differences in the curves are due to the running coupling, and become less important as p_T increases. Finally, in Fig. 6, we show the η-dependence of ρ for two values of Q_Ω for the same patch, with $p_T = 300$ GeV. The rapidity-dependence is mild for this range in η and choice of Ω.

5. Discussion

The few examples we have given in the previous section illustrate the kind of new results on energy flow that can be derived using the methods outlined in this paper. In principle, given any fixed list of jets, or heavy quarks [28], of specified momenta and directions, we may calculate the distribution of perturbative energy flow into any fixed region Ω of rapidity and azimuthal angle in the eikonal approximation. After resummation in logarithms of Q_Ω/p_T, the distribution is conveniently described in terms of the ratio $\rho(Q_\Omega/p_T)$, which specifies the percentage of events for which a transverse energy of no more than Q_Ω flows into region Ω.

The corresponding distribution, $d\rho/d\eta dp_T dQ_\Omega$ may also be interpreted as a *correlation* of transverse energy flows, between the jet cone and region Ω, generalizing energy-energy correlations [27] to "moving cone" multijet algorithms, introduced by Giele and Glover [29]. These are examples of Tkachov's "jet discriminators" [30]. In the formalism of [29], the discussion in this paper relates to a three-cone configuration, in which two cones sample high-p_T jets, while one "cone", covering Ω, encounters relatively soft radiation. We also anticipate that appropriate moments with respect to transverse energy in Ω may be analyzed in the spirit of [31], to gain insight into the influence of nonperturbative corrections for this class of correlations.

In this paper, we have investigated only the relatively simple case of valence approximation. An extension to the full range of flavor variations in $2 \to 2$ scattering, including quark-gluon and gluon-gluon scattering, will be given elsewhere [17]. Beyond this, we hope that the kind of energy flow analysis described here will provide an additional tool to study more complex jet events and production mechanisms at short distances [12].

Acknowledgements

We thank Anton Chuvakin, Chi Ming Hung, Gianluca Oderda, and Jack Smith for many very helpful conversations. We also benefited greatly from discussions of jets and energy flow with many colleagues at Snowmass 2001, including Jon Butterworth, Steve Ellis, Daniel Elvira, Brenna Flaugher, Walter Giele, Anna Kulesza, and Nikos Varelas. G.S. would like to thank Brookhaven National Laboratory for its hospitality, and C.F.B. thanks the Division of Particles and Fields of the American Physical Society for support at Snowmass 2001. This work was supported in part by the National Science Foundation, grant PHY9722101.

References

[1] D.E. Soper, *Jet observables in theory and reality*, 32nd Rencontres de Moriond, 1997, *Les Arcs 1997, QCD and high energy hadronic interactions*, p. 177; hep-ph/9706320.

[2] M.L. Mangano, *Hard scattering in high-energy QCD*, International Europhysics Conference on High-Energy Physics (EPS-HEP 99), *Tampere 1999, High energy physics*, p. 33; hep-ph/9911256.

[3] B.R. Webber, *Combining matrix elements and parton showers*, 35th Rencontres de Moriond, 2000, hep-ph/0005035.

[4] J. Huston and V. Tano, *A study of the underlying event in jet and minimum bias events*, in *The QCD and Standard Model working group: summary report, Workshop on Physics at TeV Colliders*, Les Houches, France, 7-18 Jun 1999, hep-ph/0005114.

[5] R. Field for the CDF collaboration, *The underlying event in large transverse momentum charged jet and Z-boson production*, FERMILAB-CONF-00-289-E.

[6] F. Abe *et al.* (CDF Collaboration), *Measurement of double parton scattering in $p\bar{p}$ collisions at $\sqrt{s} = 1.8$ TeV*, Phys. Rev. Lett. **79**, 584 (1997).

[7] J. Pumplin, *Hard underlying event correction to inclusive jet cross sections*, Phys. Rev. D **57**, 5787 (1998), hep-ph/9708464.

[8] J.A. Appel *et al.* (UA2 Collaboration), *Experimental study of the emergence of two-jet dominance in $p\bar{p}$ collisions at $\sqrt{s} = 630$ GeV*, Phys. Lett. **165B**, 441 (1985).

[9] F. Abe *et al.* (CDF Collaboration), *Measurement of QCD jet broadening in $p\bar{p}$ collisions at $\sqrt{s} = 1.8$ TeV*, Phys. Rev. D **44**, 601 (1991).

[10] G. Marchesini and B.R. Webber, *Associated transverse energy in hadronic jet production*, Phys. Rev. D **38**, 3419 (1988).

[11] Yu.L. Dokshitzer, V.A. Khoze, S.I. Troyan, *Coherence and physics of QCD jets*, in *Perturbative quantum chromodynamics*, ed. A.H. Mueller (World Scientific, Singapore, 1989), p. 241; Yu.L. Dokshitzer, V.A. Khoze, S.I. Troyan, *QCD coherence in high energy reactions*, Rev. Mod. Phys. **60**, 373 (1988).

[12] J.R. Ellis, V.A. Khoze and W.J. Stirling, *Hadronic antenna patterns to distinguish production mechanisms for high E(T) jets*, Z. Phys. **C75**, 287 (1997), hep-ph/9608486.

[13] V.A. Khoze and W.J. Stirling, *On the partonometry of V ($= \gamma$, W, Z) + jet events at hadron colliders*, Z. Phys. **C76**, 59 (1997), hep-ph/9612351.

[14] B. Abbott *et al.* (D0 Collaboration), *Evidence of color coherence effects in W + jets events from p anti-p collisions at $s^{\frac{1}{2}} = 1.8$ TeV*, Phys. Lett. **464B**, 145 (1999), hep-ex/9908017.

[15] G. Oderda and G. Sterman, *Energy and color flow in dijet rapidity gaps*, Phys. Rev. Lett. **81**, 3591, 1998, hep-ph/9806530.

[16] G. Oderda, *Dijet rapidity gaps in photoproduction from perturbative QCD*, Phys. Rev. D **61**, 014004, 2000, hep-ph/9903240.

[17] C.F. Berger and T. Kúcs, in preparation.

[18] J.C. Collins, D.E. Soper, G. Sterman, *Factorization of hard processes in QCD*, in *Perturbative Quantum Chromodynamics*, ed. A.H. Mueller (World Scientific, Singapore, 1989), p. 1; J.C. Collins, D.E. Soper, G. Sterman, *Factorization for short distance hadron-hadron scattering*, Nucl. Phys. **B261**, 104 (1985); J.C. Collins, D.E. Soper, G. Sterman, *Soft gluons and factorization*, Nucl. Phys. **B308**, 833 (1988); G.T. Bodwin, *Factorization of the Drell-Yan cross section in perturbation theory*, Phys. Rev. D **31**, 2616 (1985).

[19] A. Bassetto, M. Ciafaloni, G. Marchesini and A.H. Mueller, *Jet multiplicity and soft gluon factorization*, Nucl. Phys. **B207**, 189 (1982).

[20] N. Kidonakis, G. Oderda and G. Sterman, *Evolution of color exchange in QCD hard scattering*, Nucl. Phys. **B531**, 365 (1998), hep-ph/9803241.

[21] N. Kidonakis, G. Oderda and G. Sterman, *Threshold resummation for dijet cross sections*, Nucl. Phys. **B525**, 299, 1998, hep-ph/9801268.

[22] G. Sterman, *Partons, factorization and resummation - TASI 95*, Theoretical Advanced Study Institute in Elementary Particle Physics (TASI 95): *QCD and Beyond*, Boulder 1995, p. 327, hep-ph/9606312.

[23] J.C. Collins and G. Sterman, *Soft partons in QCD*, Nucl. Phys. **B185**, 172 (1981).

[24] G. Sterman, *Mass divergences in annihilation processes 2: cancellation of divergences in cut vacuum polarization diagrams*, Phys. Rev. D **17**, 2789 (1978).

[25] A. J. Macfarlane, A. Sudbery, P. H. Weisz, *On Gell-Mann's λ-matrices, d- and f-tensors, octets, and parameterizations of SU(3)*, Comm. Math. Phys. **11**, 77 (1968).

[26] H.L. Lai *et al.* (CTEQ Collaboration), *Global QCD analysis of parton structure of the nucleon: CTEQ5 parton distributions*, Eur. Phys. J. **C12**, 375 (2000), hep-ph/9903282.

[27] C.L. Basham, L.S. Brown, S.D. Ellis, S.T. Love, *Electron-positron annihilation energy pattern in quantum chromodynamics: asymptotically free perturbation theory*, Phys. Rev. D **17**, 2298 (1978).

[28] N. Kidonakis and G. Sterman, *Resummation for QCD hard scattering*, Nucl. Phys. **B505**, 321 (1997), hep-ph/9705234. N. Kidonakis, *Resummation for heavy quark and jet cross sections*, Int. J. Mod. Phys. **A15**, 1245 (2000), hep-ph/9902484; N. Kidonakis, E. Laenen, S. Moch and R. Vogt, *Sudakov resummation and finite order expansions of heavy quark hadroproduction cross sections*, hep-ph/0105041.

[29] W.T. Giele and E.W.N. Glover, *Probabilistic jet algorithms*, hep-ph/9712355.

[30] F.V. Tkachov, *Measuring the number of hadronic jets*, *Phys. Rev. Lett.* **73**, 2405 (1994), hep-ph/9901332.

[31] G.P. Korchemsky and G. Sterman, *Power corrections to event shapes and factorization*, *Nucl. Phys.* **B555**, 335 (1999), hep-ph/9902341; Yu.L. Dokshitzer, G. Marchesini and B.R. Webber, *Nonperturbative effects in the energy energy correlation*, *JHEP 9907*, 012 (1999), hep-ph/9905339; A. Banfi, G. Marchesini, G. Smye and G. Zanderighi, *Out of plane QCD radiation in hadronic Z_0 production*, hep-ph/0106278; A.V. Belitsky, G.P. Korchemsky and G. Sterman, *Energy flow in QCD and event shape functions*, hep-ph/0106308.